Journal of Hydrology 522 (2015) 618–627

Contents lists available at ScienceDirect

Journal of Hydrology

journal homepage: www.elsevier.com/locate/jhydrol

Examination of groundwater recharge with a calibrated/validated flow model of the deep vadose zone

T. Turkeltaub [a,b,*], D. Kurtzman [b], G. Bel [c], O. Dahan [a]

[a] Dept. of Hydrology & Microbiology, Zuckerberg Institute for Water Research, Blaustein Institutes for Desert Research, Ben Gurion University of the Negev, Sede Boqer Campus 84990, Israel
[b] Institute of Soil, Water and Environmental Sciences, The Volcani Center, Agricultural Research Organization, PO Box 6, Bet Dagan 50250, Israel
[c] Dept. of Environmental Physics, Blaustein Institutes for Desert Research, Ben Gurion University of the Negev, Sede Boqer Campus 84990, Israel

ARTICLE INFO

Article history:
Received 8 September 2014
Received in revised form 8 January 2015
Accepted 10 January 2015
Available online 20 January 2015
This manuscript was handled by Corrado Corradini, Editor-in-Chief, with the assistance of Rao S. Govindaraju, Associate Editor

Keywords:
Deep percolation
Vadose zone
Flow and transport model
Groundwater recharge

SUMMARY

Recharge estimations are required for efficient groundwater systems management. Better estimations could be obtained by improving our understanding of the relationship between climate factors and recharge. This study explores the calibration of a Richards' equation-based model to transient deep vadose zone data, thereby allowing simulation of groundwater recharge over long periods and an investigation of the temporal correlations between recharge and precipitation. An array of four vadose zone-monitoring systems implemented in four different slanted boreholes drilled in different orientations into a deep vadose zone sandy formation (20 m × 20 m × 20 m) enabled continuous monitoring of water content at selected depths and locations across the entire vadose zone under a Mediterranean climate. This unique high-resolution set of transient deep vadose zone data was used for inverse simulations. The flow model was then validated with a set of data under different atmospheric boundary conditions. The long-term mean annual recharge under a natural sand dune was calculated as 327 mm year^{-1}, 72% of the average annual precipitation (1996/7–2012/3), reflecting low evapotranspiration and runoff. The temporal cross-correlation analysis showed high correlations between the accumulated precipitation (over 6–9 months) and the monthly recharge after 3 to 4 months. Therefore, we conclude that the recharge fluxes are mainly influenced by the relatively recent (5–12-months) precipitation patterns. Including this time lag between precipitation and recharge, a predictive regression model was developed in which the May-to-April recharge is explained by annual precipitation in the previous year.

1. Introduction

Recharge estimations play an important role in groundwater systems management and research. The magnitude and timing of groundwater recharge are controlled by climatic and geological factors and have long been of scientific and practical interest (Ng et al., 2009; Smerdon et al., 2010; Kim and Jackson, 2012). Empirical relationships and statistical measures have been used to assess the influence of these factors on recharge (Wu et al., 1996; Kennett-Smith et al., 1994; Jan et al., 2007; Lorenz and Delin, 2007; Sheffer et al., 2010; Kim and Jackson, 2012; Wohling et al., 2012).

Unsaturated flow modeling, in which the Richards' equation is solved numerically, has been used for estimations of groundwater recharge under various conditions (Wang et al., 2009; Nolan et al., 2010; Kurtzman and Scanlon, 2011; Botros et al., 2012; Kim and Jackson, 2012; Turkeltaub et al., 2014). Solutions of the Richards' equation require knowledge of soil water retention as well as the unsaturated hydraulic conductivity function, and should be estimated under transient conditions (Hillel, 1998; Bear and Cheng, 2009). *In situ*-implemented sensors can obtain data for the state variables (e.g. water content and pressure head) in their natural environment, implicitly including interactions between different soil layers and across scales (Wollschläger et al., 2009). Inverse modeling, in which models are calibrated using measured variables, has gained popularity for estimating the hydraulic functions of the unsaturated zone. These models can then reproduce independent measurements as validation (Jacques et al., 2002; Ritter et al., 2003; Wöhling et al., 2008; Wollschläger et al., 2009; Chen et al., 2014; Turkeltaub et al., 2014).

* Corresponding author at: Dept. of Hydrology & Microbiology, Zuckerberg Institute for Water Research, Blaustein Institutes for Desert Research, Ben Gurion University of the Negev, Sede Boqer Campus 84990, Israel. Tel.: +972 8 6485012, Mobile: +972 52 3584844; fax: +972 8 6563504.
E-mail address: tuviat@post.bgu.ac.il (T. Turkeltaub).

http://dx.doi.org/10.1016/j.jhydrol.2015.01.026
0022-1694/

Development of a vadose zone-monitoring system (VMS) has enabled continuous acquisition of information on the temporal variations of the vadose zone water-content profiles (Dahan et al., 2007, 2009; Rimon et al., 2007; Baram et al., 2012, 2013; Turkeltaub et al., 2014), the chemical evolution of the pore water at multiple depths from land surface and the root zone to the water table (Dahan et al., 2009; Rimon et al., 2011a; Baram et al., 2012; Turkeltaub et al., 2014), and water pressure (Rimon et al., 2011b).

The objective of this study was to investigate the relationship between precipitation and groundwater recharge in a sand dune area. A calibrated unsaturated flow model was used to provide detailed transient deep vadose zone data and long periods of climate data. The data for the calibration process were obtained by an array of VMSs which were installed in various orientations at the sand dune site. Previous studies showed that no significant field-scale (meters) preferential flow dominates the percolation process at the site and that the subsurface is made up of relatively homogeneous and horizontal layers (Rimon et al., 2007). These conclusions were the basis for the uniform vertical unsaturated flow model that was calibrated to the VMS transient data in this work. The calibrated model allowed calculating recharge fluxes with high temporal resolution. The relationship between precipitation and recharge was then statistically analyzed at monthly and yearly resolutions.

2. Methods

2.1. Research area and instrumentation setup

The study site was located in the southern coastal plain of Israel, south of the city of Ashdod (34°38′26″E 31°46′7″N). A Mediterranean climate prevails at the study site, the summers are completely dry, and the rainy season extends from October to April, with an annual precipitation average of 450 mm (spatial interpolation of the nearest station's data provided by the Israeli Meteorological Service, 2014 [IMS]). The average temperature in the hottest month is 31.2 °C (August) and in the coldest month, 17.8 °C (January) (IMS). Reference evapotranspiration (ET) rates calculated according to the Penman–Monteith method (suggested by the Food and Agriculture Organization) range from 1.5 mm day^{-1} (January) to 5.7 mm day^{-1} (July) (IMS). The site is characterized as a sand dune area with a moderate slope. Sparse herbaceous vegetation grows in the inter-dune area, but the dunes themselves are bare sand (Fig. 1). The coarse matrix of the sand dunes in the area (98% sand in particle-size distribution analysis) promotes rapid infiltration and prevents runoff during rain events. The shallow stratigraphy consists of Holocene sand dunes, calcareous sandstone, and clayey interlayers (Ecker, 1999). Rainwater infiltration through the sand dune recharges the phreatic sandy coastal aquifer. The water table at the monitored site is approximately 21 m below ground surface.

Four VMSs were installed at the sand dune site, enabling continuous measurements of water contents at multiple depths using 15 flexible time-domain reflectometry (FTDR) sensors. Two of the VMSs were instrumented with vadose zone pore water-sampling ports (VSPs) which were used for either frequent sampling of the vadose zone pore water or measuring the pressure head at multiple depths. The system has been previously described (Dahan et al., 2009; Rimon et al., 2011a); herein we provide a brief overview of the system for completeness. The monitoring system is composed of a flexible sleeve made of a thin polyvinyl chloride liner, hosting several customized FTDR probes (Dahan et al., 2003) for water-content measurements and VSPs (Rimon et al., 2011a). The monitoring systems were installed in uncased, small-diameter (15 cm), slanted (35°) boreholes penetrating the 21-m

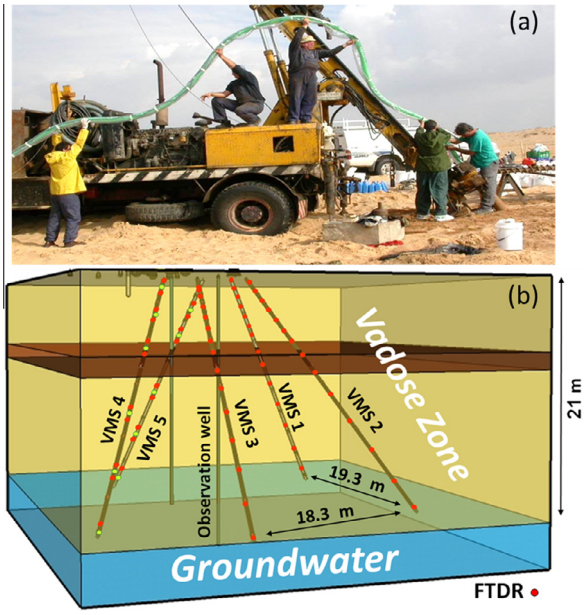

Fig. 1. The sand-dune site: (a) the drilling rig during the installation of the long flexible vadose-monitoring system (VMS; green) in the slanted borehole. (b) The VMSs in their different orientations in the slanted boreholes and location of the observation well (modified from Rimon et al., 2007). (For interpretation of the references to color in this figure legend, the reader is referred to the web version of this article.)

thick vadose zone of the study site. Consequently, the FTDR probes and VSPs were aligned along the slanted borehole's upper sidewall facing the undisturbed sediment column, which extended from the probe location on the top wall of the borehole to land surface. Each of the probes and sampling ports represents a different undisturbed profile because every probe and sampling port is shifted both vertically and horizontally from the next. Vertical boreholes were drilled next to the VMSs for accurate sediment sampling. Particle-size distributions of these samples were analyzed by hydrometer method (Klute, 1986). One of these boreholes was then completed as a piezometer with a screen interval of 5 m below the water table.

2.2. Model setup

To have an accurate tool for analyses of the precipitation–recharge relationship, a calibrated unsaturated flow model was used for groundwater-recharge simulations. The Richards' equation was implemented to account for water flow in the vadose zone of the sand dune, and the unsaturated hydraulic functions of the different layers were described by the van Genuchten–Mualem formulation (Mualem, 1976; van Genuchten, 1980). The parameters of the hydraulic functions were inversely calculated by the HYDRUS-1D code (Šimůnek et al., 2009) which numerically simulates the 1D form of the Richards' equation and includes a Marquardt–Levenberg-type (Marquardt, 1963) parameter-optimization algorithm for inverse estimation.

The sand-dune model was calibrated to transient data from the deep vadose zone. These data contained temporal and spatial variations in the water contents of the deep vadose zone at multiple depths and locations. These variations are a consequence of rainwater infiltration into the soil and drainage of the unsaturated zone down to the phreatic aquifer. The hydraulic properties of the layers in the modeled domain were defined according to particle-size distribution analyses as well as measured water contents.

The model's domain was discretized into 250 nodes, with a finer grid close to the surface. The number of nodes and density of the

upper side of the grid were fixed when there were no further improvement in results and the numerical solution showed stability (coverage for numerous combinations of parameters).

2.3. Boundary and initial conditions

Atmospheric boundary conditions were set at the upper boundary (land surface). This boundary condition changes from prescribed flux to prescribed head condition and vice versa, according to the precipitation, potential ET and subsurface conditions. Precipitation, potential ET, and the minimum allowed pressure head at the soil surface that permits evaporation (hCritA) (see HYDRUS-1D User Manual, Šimůnek et al., 2009) were introduced into the top boundary at daily temporal resolution. This time resolution was imposed by the availability of the meteorological data. The sand dune-modeled column extended to a depth of 19 m (~1.5 m above the water table). Thus, the lower boundary condition was prescribed as a free-drainage boundary condition (unit gradient flow). The initial water-content profile was set to the measured water contents at the different moisture sensors, on the date at which the model runs were initiated.

Daily measurements of precipitation and calculated reference ET were provided by the IMS and Israeli Ministry of Agriculture. Spatial interpolation of precipitation data was used to estimate the daily precipitation at the sand dune. The inverse distance weighted (IDW) method was used for spatial interpolation:

$$\widehat{R}_0 = \frac{\sum_i^n \frac{R_i}{D_{0i}^p}}{\sum_i^n \frac{1}{D_{0i}^p}} \quad (1)$$

where $\widehat{R}_0$ is the estimated precipitation in the unsampled location, R_i is the precipitation measured at point i, D_{0i} is the distance between the estimated location 0 and the measured point i, n is the number of measured points used for estimating the precipitation at point 0, and p is the IDW exponent that controls the difference in relative weights of closer and further measurement points (i.e. higher exponents indicate higher weights for closer measurements) (Kurtzman et al., 2009).

2.4. Inverse modeling

The effective hydraulic parameters of the unsaturated zone layers were determined by inverse modeling of daily observed water contents acquired by the VMSs at selected depths and locations. These data were monitored by 11 FTDR sensors for 350 days (3850 point measurements overall). The inverse estimation was conducted by minimizing the objective function (Šimůnek et al., 2009):

$$\Phi(\theta; b|c) = \sum_{i=1}^{m} [\theta_{obs}(t_i) - \theta_{sim}(t_i, b|c)]^2 \quad (2)$$

where m is the number of observations, θ_{obs} and θ_{sim} are measured and simulated volumetric water contents, $b|c$ is the vector b (see explanation further on) containing the unknown parameters estimated given the fixed and known parameters in vector c. The weight for an individual observation was assumed to be equal to 1.

The model was constructed of eight layers with six van Genuchten–Mualem parameters each. Since, hydraulic experiments depend on $\Delta\theta = \theta s$ (saturated water content) – θr (residual water content), and not on each parameter individually (Wollschläger et al., 2009), the θr parameters were estimated by particle size distribution and Rosetta (Schaap et al., 2001), and were fixed throughout the inverse process. l (pore connectivity and tortuosity factor), which showed to be unimportant or insensitive in numerical and real data experiments (e.g. Wang et al., 2009; Wollschläger et al., 2009), were fixed for all layers (Tables 1 and 2). For layers 4 and 8, θs (saturated water content) was fixed as well (Tables 1 and 2). The remaining 30 parameters were used for calibration. Due to the large number of parameters and the limited number of parameters that could be optimized (15 parameters, limited by HYDRUS), the inverse-modeling process was divided into two stages (Fig. 2). First, the parameter vector $b = \{\theta s, \alpha, n, K_s\}$ for model layers 1–4 (θs of layer 4 was fixed) was optimized, while the 32 other parameters were fixed (vector c). Then the optimized parameters of layers 1–4 were fixed (becoming the new vector c) in the HYDRUS-1D code and the parameter vector $b = \{\theta s, \alpha, n, K_s\}$ for model layers 5–8 (θs of layer 8 was fixed) was optimized. Then, the optimized parameters of layers 5–8 were fixed, and the parameters of layers 1–4 were optimized again (large loop in Fig. 2). Thus, to reach convergence of the parameters, the procedure was executed in cycles. These cycles were terminated when the parameters' weighted average (see below) did not change compared with the weighted average of earlier runs.

Uniqueness and stability of the inverse solution were tested by solving the inverse problem repeatedly using different combinations of random initial parameter values (Fig. 2). These values were randomly sampled from the parameters' ranges, which were bounded at the beginning of the runs to limit the inverse solution (Table 1). Thus, in each calculation, different initial parameters started the inverse process. For example, the parameter vector $b = \{\theta s, \alpha, n, K_s\}$ for model layers 1–4 that contained 15 parameters was optimized multiple times. Each time, there were 15 random values of parameters starting the inverse calculation. The output of each calculation was saved. At the end of multiple runs, the inverse solution with the lowest sum of squares (ssq) was pursued by going through the output files. Most of the inverse solutions reached to similar low ssq values ($0.012 < ssq < 0.021$, 96% for 1–4 layers and $0.016 < ssq < 0.025$, 93% for 5–8 layers). Parameter distributions were analyzed in order to confirm that the simulations with the low ssq reached similar parameter values and thus represent the global minimum of the ssq. Although some of the optimized parameters obtained similar values throughout the inverse simulations, others presented wider uncorrelated distributions. Therefore, in order to allow greater influence to simulations with the lower ssq and to extract all the information provided by the inverse process, the final parameters were calculated according to:

$$\overline{A} = \frac{1}{\sum_{i=1}^{i} \frac{1}{ssq_i}} \sum_{i=1}^{i} A_1 \times \frac{1}{ssq_1} + A_2 \times \frac{1}{ssq_2} + \ldots + A_i \times \frac{1}{ssq_i} \quad (3)$$

where A_i is the parameter value of specific inverse solution, $\overline{A}$ is parameter weighted average and ssq_i is sum of squares of specific inverse solution. In addition, sensitivity tests were conducted for the parameters and found that varying the parameters within the provided confidence interval does not significantly affect the results.

Two types of validation runs were performed for the calibrated flow model: (i) with available observations from the same 11 sensors that were used for calibration, which were constrained to different initial and atmospheric boundary conditions in different observation years (~335 daily measurements × 11 FTDR measurement points); (ii) with an additional four sensors, which were not included in the calibration runs (~700 daily measurements × 4 FTDR measurement points). The deviations from 365 and 730 days were due to unreliable or no data collection on some days due to technical problems.

2.5. Exploratory statistical analysis

The temporal variability of the recharge and its relation to precipitation was investigated by cross-correlation statistical analysis.

Table 1
The van Genuchten–Mualem parameters bounds used in the inverse calculations for the model's eight layers. The residual water contents (θr) and l parameter (0.5) were held constant throughout the inverse simulations for all layers. For layers 4 and 8, the saturated water content (θs) was held constant.

Layer	θs	α (cm^{-1})	n (–)	Ks (cm day^{-1})	Number of nodes	Discretized depth (cm)
Top						
Layer 1	[0.33…0.4]	[0.03…0.2]	[2.5…4]	[1000…2000]	27	0–102.3
Layer 2	[0.33…0.4]	[0.03…0.2]	[2.5…4]	[1000…2000]	44	106.7–326.6
Layer 3	[0.33…0.4]	[0.03…0.2]	[2.5…4]	[1000…2000]	37	332.4–564.7
Layer 4		[0.03…0.2]	[2.5…4]	[1000…2000]	24	571.8–735.7
Bottom						
Layer 5	[0.37…0.43]	[0.03…0.1]	[1.3…2.5]	[0.1…150]	11	743.5–823.6
Layer 6	[0.37…0.43]	[0.03…0.1]	[1.5…2.5]	[1…400]	26	831.8–1047.4
Layer 7	[0.33…0.4]	[0.03…0.2]	[2.5…4]	[1000…2000]	39	1056.5–1425.1
Layer 8		[0.03…0.1]	[1.3…2.5]	[1…400]	42	1435.5–1900

Table 2
The optimized effective hydraulic van Genuchten–Mualem parameters. 'Top' represents the first 7 m (sandy formation) and 'Bottom' represents the rest of the soil column.

Layer	Vertical depth (m)	θr	θs	α (cm^{-1})	n (–)	Ks (cm day^{-1})
Top						
Layer 1	0–1	0.055	0.362	0.127	2.52	1464.4
Layer 2	1–3.2	0.055	0.39	0.136	2.86	1721.6
Layer 3	3.2–5.7	0.055	0.35	0.13	2.93	1756.24
Layer 4	5.7–7.3	0.055	0.35	0.11	2.79	1069.5
Bottom						
Layer 5	7.3–8.3	0.07	0.43	0.038	1.4	40.8
Layer 6	8.3–10.4	0.07	0.4	0.065	1.52	254.8
Layer 7	10.4–14.3	0.055	0.347	0.16	2.18	1416.3
Layer 8	14.3–19	0.07	0.38	0.067	1.52	336.7

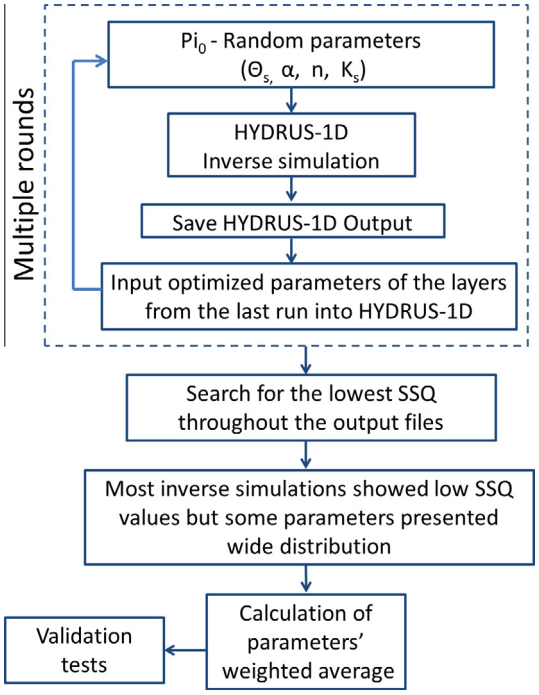

Fig. 2. Work flow of the inverse modeling. The parameter values were randomly sampled from the parameter ranges, which were bounded at the beginning of the runs to limit the inverse solution. SSQ – sum of squares.

Cross-correlation analysis reveals the relevant period of cumulative precipitation and the response time of the recharge fluxes to precipitation. Due to the relatively large depth of the investigated vadose zone (~20 m), positive cross-correlation between the monthly precipitation and the monthly recharge is expected to be rather poor. Recharge is more likely to be related to the cumulative precipitation. Hence, analysis included the cross-correlations between cumulative precipitation (including the special case of monthly precipitation) and monthly recharge. The cumulative precipitation was calculated as the sum of successive monthly precipitation values:

$$CP(t,\Delta) = \sum_{t-\Delta+1}^{t} P(t-\Delta) + \ldots + P(t), \tag{4}$$

where $CP(t,\Delta)$ is the cumulative precipitation (mm $(\Delta$ month$)^{-1}$), P is monthly precipitation (mm $month^{-1}$) and Δ is the number of successive months.

A delay between the precipitation and the recharge response is expected. Therefore, we calculated the cross-correlation by varying two parameters—the period over which the precipitation was accumulated, Δ, and the delay between the end of the accumulation period and the observed response of the recharge, τ. The cross-correlation function of these two variables was defined as:

$$CC(\tau,\Delta) = \frac{\frac{1}{N-\tau}\sum_{1}^{N-\tau}\left[Re(t+\tau)-\overline{Re}\right]\left[CP(t,\Delta)-\overline{CP(\Delta)}\right]}{\sqrt{var(Re)}\sqrt{var(CP)}} \tag{5}$$

where $CC(\tau,\Delta)$ is the cross-correlation coefficient, Re is the monthly recharge flux (mm $month^{-1}$), $\overline{Re}$ is the mean monthly recharge, $CP(t,\Delta)$ is the cumulative precipitation per Δ months (mm $(\Delta$ month$)^{-1}$), and $\overline{CP(\Delta)}$ is the mean cumulative precipitation per Δ months (mm $(\Delta$ month$)^{-1}$).

Finally, a regression model was developed to evaluate the recharge. Due to the low evaporation and runoff, the regression model was based on precipitation factors. Four variables were examined: annual precipitation, maximum yearly storm event, number of wet days, and number of dry days between storms. The proposed form of the regression equation was:

$$R = \alpha_0 + \alpha_1 X_1 + \cdots + \alpha_4 X_4 \tag{6}$$

where R is the estimated annual groundwater recharge, $\alpha_0 \ldots \alpha_n$ are regression coefficients, and the $X_j s$ are the aforementioned precipitation-related variables.

3. Results and discussion

3.1. Dynamics of the deep-percolation process

A comprehensive description of the percolation and transport processes across the vadose zone of the site was given by Rimon et al. (2007, 2011a). Nevertheless, data obtained from 2006/7 are presented here to extend the reader's understanding of the characteristics of the data that were used in the inverse simulations to estimate the effective parameters. To avoid data overload, representative FTDRs located at 7 (out of 15) depths across the vadose zone were chosen to demonstrate the percolation dynamics induced by precipitation (Fig. 3). Rimon et al. (2007) dedicated a full chapter to show resembles of hydraulic response of sensors from similar depths to the percolation events. In the upper sandy layers (<7.3 m), most of the significant rain events initiated an infiltration wave that propagated down the vadose zone, expressed as a rise in water content upon arrival of a wetting front followed by reduction in water content during a drainage phase (Fig. 3a). In contrast, FTDRs located in the finer-grained sandy-loam layer in deeper sections tracked a single long annual rise in water content that started upon arrival of a wetting front, then gradually decreased during the later drainage phase (Fig. 3b).

3.2. Inverse simulations

The sand-dune model was calibrated according to transient data obtained from the entire vadose zone (~20 m). These data sets of water-content measurements were obtained from Sep 2006–Sep 2007 by 15 FTDRs located at different positions and depths in the vadose zone of the sand dune (Figs. 3–5). Data sets which were obtained from Sep 2007–Sep 2008 were used for validation, along with data sets from other FTDRs which were not included in the inverse simulations (Fig. 6).

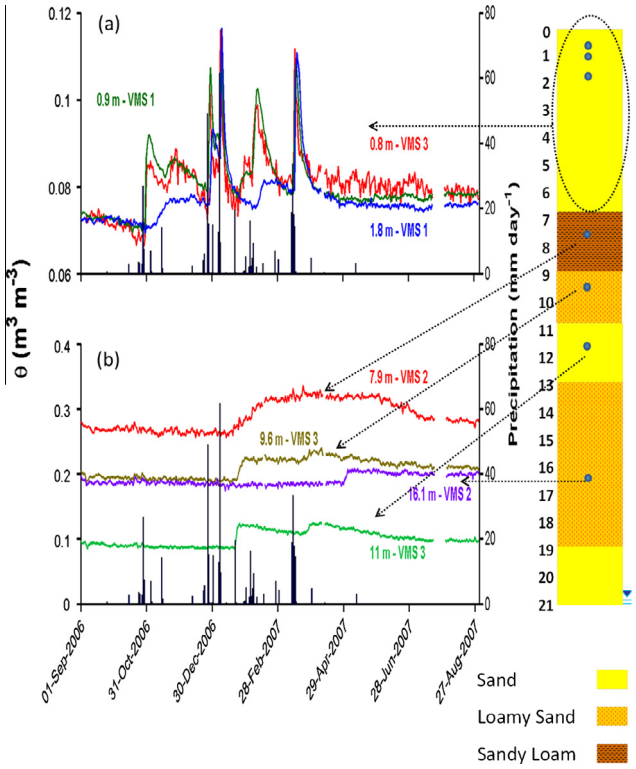

Fig. 3. Daily rainfall and water-content variations at different depths across the vadose zone as monitored by the vadose-zone monitoring systems (VMSs) (see Fig. 1 for VMS #): (a) water content variation in the upper 7 m, and (b) water content variation at depths of 7–16.1 m.

The inverse simulations resulted in a model composed of eight layers extending 19 m in depth and 30 optimized parameters (Table 2). The top four layers were characterized by a sandy texture and shared similar hydraulic properties (top interval, Table 2, Fig. 3). After multiple trials, the sandy zone was optimally divided into four layers to achieve the best fit between the simulated and observed water-content profiles. Under the sandy layers, the vadose zone was composed of four layers that exhibited variable hydraulic properties (bottom interval, Table 2, Fig. 3).

Data from eight FTDRs at depths of 0.9 m, 1.8 m, 2.2 m, 3.4 m, 3.8 m, 6 m, 3 m and 5.5 m (the latter two were not part of the calibration process) were chosen to demonstrate the calibration and validation fit of the model in the top interval (sandy layers) of the vadose zone (Figs. 4 and 6a,b). It is worth reiterating that due to the slanted installation of the VMS, each depth measures an independent vertical sediment column, that is, the FTDRs are shifted vertically and horizontally away from each other. Thus the data points should be regarded as arbitrarily distributed in a 3D vadose zone domain rather than in a single vertical profile. The data and the model in the top interval displayed simultaneous rises in water contents following rain events, indicating an adequate temporal description of the water flow by the model. Nevertheless, there were some discrepancies between the modeled and observed water contents during the arrival of the wetting front. For example, the modeled water content peaks were always higher than the measured ones. This disagreement between model and measurement might result from the unaccounted-for heterogeneity of the soil layers, the temporal resolution of the model, or a combination of these. In addition, while the model represents a point in the modeled domain, the FTDR measures an average value over a larger volume which is slightly disturbed by the VMS structure (Rimon et al., 2011a). Therefore, a slight deviation between the measured water content and the modeled values is expected, especially during dynamic flow stages.

The calibration and validation of the model in the bottom part of the vadose zone are represented by five FTDR sensors at depths of 7.9 m, 9.6 m, 11 m, 14.6 m and 16.1 m (Fig. 5) and another two FTDR sensors that were not part of the calibration at depths of 9.1 m and 11 m (Fig. 6c and d). Here as well, most of the observed and modeled data displayed simultaneous rises in water contents. However, close inspection of the goodness of fit between simulated and observed data revealed discrepancies concerning the arrival of the wetting front in both calibration and validation. At 7.9 m depth, where the clay content of the sediment is significantly higher (23%) than the rest of the layers (Fig. 5a and b), during the calibration, the simulated wetting front preceded the observed one by 17 days. Moreover, the second peak which was simulated by the model was not measured by this FTDR sensor, whereas with the deeper FTDR sensors, the second peak was observed and simulated (Fig. 5c and e). For the validation results, the model simulated an early small increase in water content that was not measured by the FTDR sensor (Fig. 5b), but the high peak arrival was within the same time frame as the measured increase in water content. At 9.6 m depth (Fig. 5c and d), during calibration, the simulated wetting front preceded the observed one by 10 days. Nevertheless, at 9.1 m depth (Fig. 6c), which was not included in the calibration, the simulated and observed water contents displayed simultaneous rises in water contents. During validation, there were no such discrepancies. An interesting situation occurred at 16.1 m depth (Fig. 5i and j), where in the validation run, the model adequately simulated the observed data, whereas the calibration results were poor. These variations might be attributed to the natural heterogeneity which creates minor local discrepancies between some of the measurements, even though those measure-

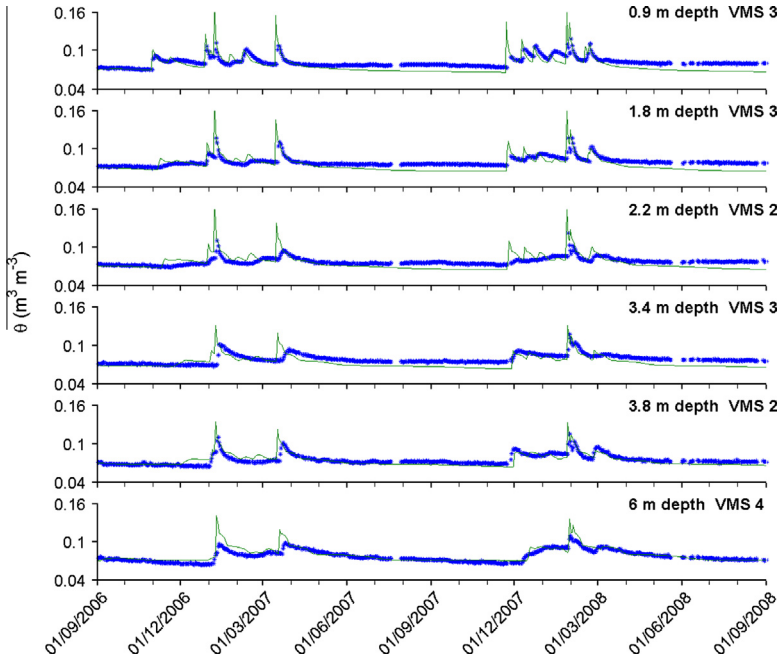

Fig. 4. Flow-model calibration (left) and validation (right) in the top 7 m. Observed water contents obtained by the FTDR sensors under the sand dune (blue points) and simulated water contents obtained with the calibrated model (green line). (For interpretation of the references to color in this figure legend, the reader is referred to the web version of this article.)

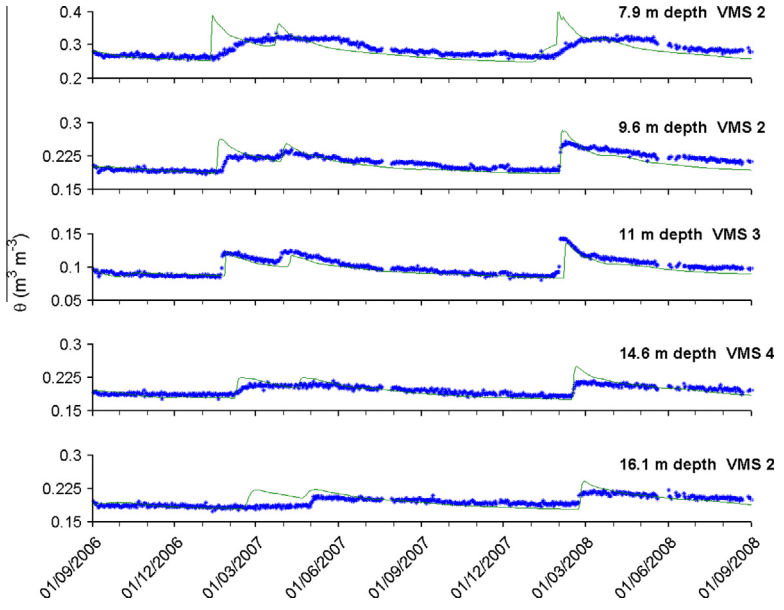

Fig. 5. Flow-model calibration (left) and validation (right) at depths greater than 7 m. Observed water contents obtained by the FTDR sensors under the sand dune (blue points) and simulated water contents obtained with the calibrated model (green line). (For interpretation of the references to color in this figure legend, the reader is referred to the web version of this article.)

ments are taken under different profiles that are located several meters apart (Fig. 1). Nevertheless, one can conclude that, in general, the model is robust, and the validation using points that were not used for the calibration showed an impressive fit (Fig. 6).

Calibration and validation indicated that the 1D classical Richards' equation can capture the major phenomena revealed in the monitoring data obtained from the 3D thick vadose zone. Nevertheless, discrepancies and the model's inability to fully describe the obtained data stemmed from a gap between scales—the measurements representing bigger volumes than the model—and disincorporation of more complex processes.

3.3. Recharge estimation

The groundwater recharge under the sand dune was simulated using 17 years of meteorological data (1996–2013) at a daily resolution as the top boundary of the model. Previous studies have shown that uncertainty in one of the van Genuchten parameters might lead to uncertainty in recharge estimations (Nolan et al., 2007; Wang et al., 2009). Therefore, possible perturbation of the optimized parameters in the annual average recharge calculation was examined with a stochastic approach. This included sampling from sets of random parameters' values in each forward solution.

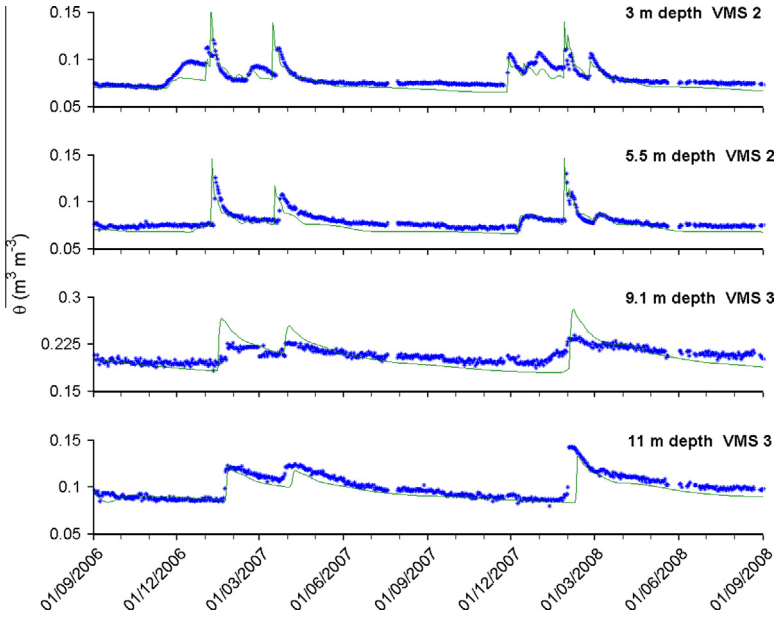

Fig. 6. Flow model and validation at FTDR sensors that were not used in the calibration process. Observed water contents (blue points) and simulated water contents obtained with the calibrated model (green line). (For interpretation of the references to color in this figure legend, the reader is referred to the web version of this article.)

The sets were contained random values within the range of ± 5% of the parameters' weighted average normalized to the difference between the prescribed boundaries (Table 1). Simulations of the recharge corresponding to each set of parameters and subject to the same top-layer boundary condition (based on the meteorological data) were performed for 1000 times. The distribution of groundwater recharge calculated for different sets of parameters is summarized in a histogram (Fig. 7).

A high average annual recharge (over 17 years) was estimated by the model under the sand dune (Table 3). The absence of vegetation and the relatively small loss of water to evaporation and surface runoff led to the high recharge rate (Table 3). Similar high fluxes under sandy soils have been reported in previous studies (Keese et al., 2005; Wang et al., 2009). Sandy areas constitute a significant and important contribution for outcrops to groundwater resources. Furthermore, the perturbation test resulted in a relatively narrow range of recharge values, from 324 to 338 mm year^{-1}. The most frequent recharge flux was 330 mm year^{-1}, 3 mm year^{-1} lower than the estimated mean (Table 3, 0.92% bias). These results showed that the parameters of the hydraulic functions, within the confidence-level range obtained from the calibration to the data, have a small influence on long-term recharge rates.

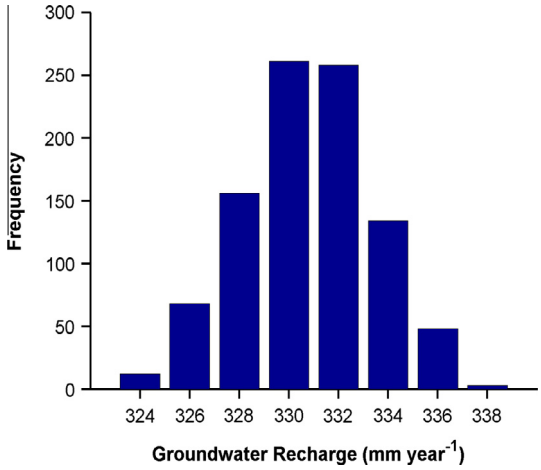

Fig. 7. Seventeen-year average of yearly groundwater-recharge distribution as calculated by 1000 simulations. In each simulation, sets of random parameters' values were sampled. The sets were contained random values within the range of ± 5% of the parameters' weighted average normalized to the difference between the prescribed boundaries. Bin size: 2 mm year^{-1}.

Table 3
Precipitation and groundwater-recharge statistics obtained by running the calibrated model with 17 years of meteorological data (1996–2013).

	Precipitation (mm year^{-1})	Recharge (mm year^{-1})
Average	450	327
Percentage	72%	
StD	101	97.8
CV	22	29.9

Average – average precipitation or recharge.
Percentage – average annual recharge percentage of average annual precipitation.
StD – standard deviation.
CV – coefficient of variation (%).

3.4. Temporal variation of recharge

The correspondence between rain depth and recharge under thick vadose zones is rather obscure. It is difficult to identify the dominant characteristic of the precipitation affecting the recharge. In this study, due to the high resolution of the calibrated flow model, it was possible to comprehensively investigate the relationships between several precipitation characteristics and groundwater-recharge patterns under the thick vadose zone.

The daily groundwater-recharge rates, which were extended over 6239 days, demonstrated the transient nature of the recharge (Fig. 8). In nearly every year, the recharge flux peaked, albeit at different amplitudes, and then declined. Moreover, the peak's arrival time during the year varied significantly (Fig. 8). Years with very low annual precipitation showed negligible recharge peaks, e.g. 1998/9 with 215 mm year^{-1} (Fig. 8).

The temporal cross-correlation between the cumulative precipitation and the monthly recharge was analyzed to describe the pre-

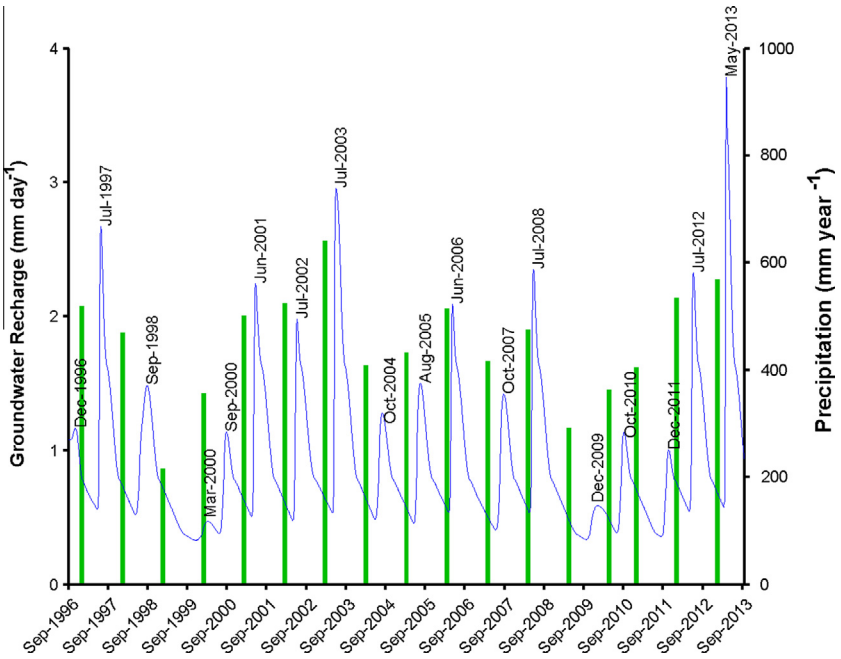

Fig. 8. Annual precipitation (green bars) and daily simulated groundwater-recharge rates at 19 m under the sand dune (blue line). Months in which the recharge rates peaked are noted. (For interpretation of the references to color in this figure legend, the reader is referred to the web version of this article.)

cipitation–recharge relationship. The cross-correlation analysis was carried out from zero cumulative precipitation (205 pairs) to 12 months' cumulative precipitation (193 pairs) and a maximum 12-month delay (Fig. 9). The highest positive temporal correlation was between 6 and 9 months of cumulative precipitation and 3–4 months of delay (lag time) in monthly recharge (Fig. 9). This means, for example, that the occurrence of a recharge peak in July was related to the cumulative precipitation during the 5–8 months ending in April (effectively the precipitation accumulated over the entire rainy season). There was a negative correlation during the 0–3 months of delay and 0–5 months of cumulative precipitation (Fig. 9, bottom left and right). This negative correlation was related to a seasonal effect. During the rainy season (October–April), recharge was usually relatively low because the rain of the previous rainy season no longer affected the recharge and the rain of the concurrent season was not yet affecting the recharge.

Despite the relative thickness of the vadose zone under this natural dune site, the recharge fluxes were mainly influenced by relatively recent precipitation patterns (5–12 months). The impact of soil water stored in previous years was small compared to that reported in previous studies conducted under similar semiarid conditions but with a finer top-soil texture and a variety of land uses (Ng et al., 2009; Turkeltaub et al., 2014).

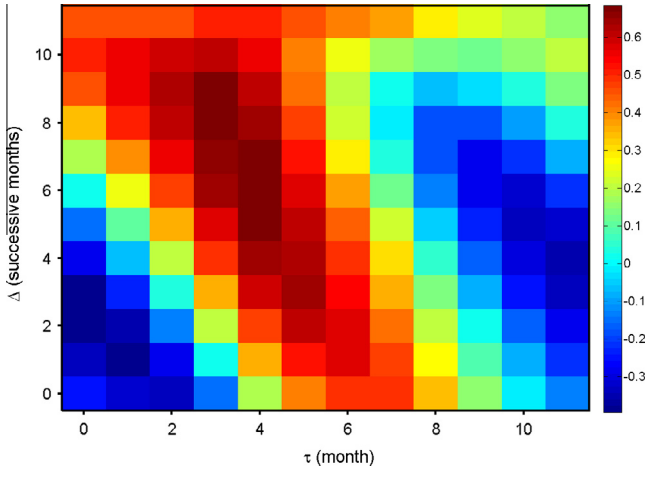

Fig. 9. Cross-correlation matrix of cumulative precipitation versus recharge flux. The horizontal axis is the lag time (month) and the vertical axis is the number of successive months over which the precipitation has accumulated. Color correspondence to correlation coefficient values is shown on the right (see Eq. (5)). (For interpretation of the references to color in this figure legend, the reader is referred to the web version of this article.)

3.5. Regression model

Once it was understood that the recharge is well correlated with the cumulative precipitation of the previous rainy season, a simple predictive model was developed for the annual recharge, starting at the end of the winter (1 May). The explanatory variables included: annual precipitation, number of rainy days, maximal rain event and annual precipitation of previous years. It is important to note that the annual precipitation and maximal rain event were highly correlated ($r = 0.84$). A 17-year analysis showed that a model in which annual precipitation is the single explanatory variable was the most significant ($r = 0.96$). A low correlation was calculated between groundwater recharge and annual precipitation of previous years ($r = 0.24$) and between groundwater recharge and number of rainy days ($r = 0.48$).

The model in which the May-to-April recharge was explained by the recent winter precipitation was compared to a simultaneous precipitation–recharge model in which October-to-September recharge was explained by precipitation during the same period; the correlation and fit between annual precipitation and annual recharge calculated from the time-lagged May-to-April model were clearly higher ($r = 0.96$, $P = 2.1E{-}9$ vs. $r = 0.87$, $P = 6.8E{-}6$, Fig. 10). Thus, recharge-estimation regression models for aquifers under a thick vadose zone must take the lag time into account. A consideration of the vadose zone as being in a steady state, with any volume of percolated water simultaneously giving the same volume of recharge at the water table—as is often practiced in groundwater models—is not valid; the time lag between the

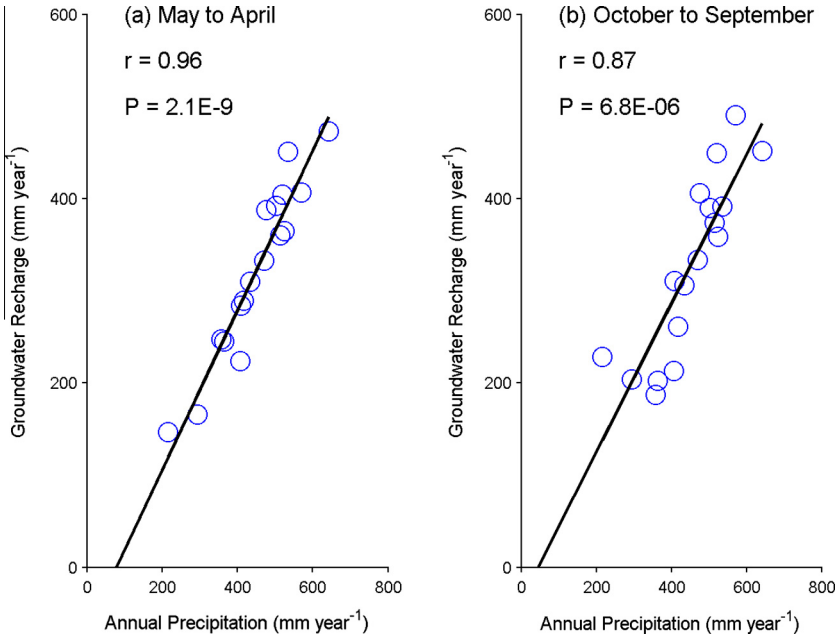

Fig. 10. Linear regression between annual precipitation and groundwater recharge (see Eq. (6)). (a) Lagged model in which groundwater recharge from May to April was calculated from annual precipitation prior to the recharge year. (b) A simultaneous model in which October-to-September recharge is explained by precipitation during the same period.

recharge and the precipitation, as well as the importance of the cumulative precipitation rather than the instantaneous one, should be considered in recharge estimations.

The linear relationship between the annual precipitation and annual groundwater recharge, with $r = 0.96$ and $P = 2.1\text{E}{-9}$ takes on the form:

$$Re = 0.86 \times (P_{annual} - 67.3)$$

where Re is the annual groundwater recharge (1 May–30 April), in mm year^{-1}, and P_{annual} is the annual precipitation prior to 1 May. This model can be used for annual groundwater-recharge estimations at any site above the coastal aquifer which is characterized by similar land, soil and vadose zone properties (bare surface and sand particle size (>95%)).

The significance of annual precipitation as explanatory variable for groundwater recharge estimation was reported in earlier studies (e.g. Sheffer et al., 2010; Kim and Jackson, 2012). Yet, the correlation between annual precipitation and groundwater recharge was not as high as in the current study. Therefore other explanatory variables, for example, soil texture (Wohling et al., 2012) which related to site characteristic, were added to the regression model.

4. Summary and conclusions

The relationship between precipitation and groundwater recharge was investigated using a calibrated Richards' equation-based model to detail the transient deep vadose zone data and perform an exploratory statistical analysis. An array of four VMSs implemented under a sand dune above the coastal aquifer of Israel provided transient data of sediment water content at selected depths and locations throughout the entire vadose zone (~20 m × 20 m × 20 m). The high-resolution transient deep vadose zone data were used for inverse simulations of the unsaturated flow model. The flow model was then validated with a set of data collected under different atmospheric boundary conditions.

The long-term mean annual recharge under the natural sand dune was calculated as 327 mm year^{-1}, 72% of the average annual precipitation (1996/7–2012/3), reflecting low ET and runoff. Moreover, stochastic analysis demonstrated the low sensitivity of the recharge, as simulated by the model, to the optimized parameters of the hydraulic functions.

Investigation of the temporal variation in recharge with model simulations demonstrated that the recharge flux under a thick vadose zone is rather transient. Nearly every year, the recharge flux reaches a peak with variable arrival time. The temporal cross-correlation of the cumulative precipitation with the monthly recharge is between 6–9 months of cumulative precipitation (the cumulative precipitation during the whole rainy season) and a 3- to 4-month delay in monthly recharge.

Taking into account the lag between precipitation and recharge, a predictive regression model was developed in which the May-to-April recharge is explained by the annual precipitation for the previous year. This predictive model was found to be superior to the simultaneous precipitation–recharge model commonly considered in groundwater modeling.

Acknowledgments

The work was partly funded by the Israel Water Authority (#4500687174) and the Israeli Science Foundation (#468/04). We would like to express our appreciation to Michael Kogel for his extensive efforts in maintaining and operating the VMS. We express special gratitude to Yaara Rimon for her significant contribution to this study.

References

Baram, S., Kurtzman, D., Dahan, O., 2012. Water percolation through a clayey vadose zone. J. Hydrol. 424–425, 165–171. http://dx.doi.org/10.1016/j.jhydrol.2011.12.040.

Baram, S., Ronen, Z., Kurtzman, D., Kulls, C., Dahan, O., 2013. Desiccation-crack-induced salinization in deep clay sediment. Hydrol. Earth Syst. Sci. 17, 1533–1545. http://dx.doi.org/10.5194/hess-17-1533-2013.

Bear, J., Cheng, H.-D.A., 2009. Modeling Groundwater Flow and Contaminant Transport. Springer.

Botros, F.E., Onsoy, Y.S., Ginn, T.R., Harter, T., 2012. Richards equation-based modeling to estimate flow and nitrate transport in a deep alluvial vadose zone. Vadose Zone J. 11 (4). http://dx.doi.org/10.2136/vzj2011.0145.

Chen, M., Willgoose, G.R., Saco, P.M., 2014. Spatial prediction of temporal soil moisture dynamics using HYDRUS-1D. Hydrol. Processes 28, 171–185. http://dx.doi.org/10.1002/hyp.9518.

Dahan, O., McDonald, E.V., Young, M.H., 2003. Flexible time domain reflectometry probe for deep vadose zone monitoring. Vadose Zone J. 2, 270–275. http://dx.doi.org/10.2113/2.2.270.

Dahan, O., Shani, Y., Enzel, Y., Yechieli, Y., Yakirevich, A., 2007. Direct measurements of floodwater infiltration into shallow alluvial aquifers. J. Hydrol. 344, 157–170. http://dx.doi.org/10.1016/j.jhydrol.2007.06.033.

Dahan, O., Talby, R., Yechieli, Y., Adar, E., Lazarovitch, N., Enzel, Y., 2009. In situ monitoring of water percolation and solute transport using a vadose zone monitoring system. Vadose Zone J. 8, 916–925. http://dx.doi.org/10.2136/vzj2008.0134.

Ecker, A., 1999. Atlas of selected geological cross-sections and subsurface maps in the coastal aquifer of Israel. Israel Geol. Surv., Jerusalem.

Hillel, D., 1998. Environmental Soil Physics, first ed. Academic Press, Elsevier, New York.

Israel Meterological Service, 2014. Web Israel Meteorological Service: Data base. <http://data.gov.il/ims-results> (accessed 01.04.14).

Jacques, D., Šimůnek, J., Timmerman, A., Feyen, J., 2002. Calibration of Richards' and convective-dispersion equations to field-scale water flow and solute transport under rainfall conditions. J. Hydrol. 259, 15–31. http://dx.doi.org/10.1016/S0022-1694(01)00591-1.

Jan, C.-D., Chen, T.-H., Lo, W.-C., 2007. Effect of rainfall intensity and distribution on groundwater level fluctuations. J. Hydrol. 332, 348–360. http://dx.doi.org/10.1016/j.jhydrol.2006.07.010.

Keese, K.E., Scanlon, B.R., Reedy, R.C., 2005. Assessing controls on diffuse groundwater recharge using unsaturated flow modeling. Water Resour. Res. 41, W06010. http://dx.doi.org/10.1029/2004WR003841.

Kennett-Smith, A., Cook, P.G., Walker, G.R., 1994. Factors affecting groundwater recharge following clearing in the south western Murray Basin. J. Hydrol. 154, 85–105. http://dx.doi.org/10.1016/0022-1694(94)90213-5.

Kim, J.H., Jackson, R.B., 2012. A global analysis of groundwater recharge for vegetation, climate, and soils. Vadose Zone J. 11. http://dx.doi.org/10.2136/vzj2011.0021RA.

Klute, A. (Ed.), 1986. Methods of soil analysis. Part 1. Agron. Monogr., vol. 9. ASA and SSSA, Madison, WI.

Kurtzman, D., Navon, S., Morin, E., 2009. Improving interpolation of daily precipitation for hydrologic modelling : spatial patterns of preferred interpolators. Hydrol. Processes 23, 3281–3291. http://dx.doi.org/10.1002/hyp.7442.

Kurtzman, D., Scanlon, B.R., 2011. Groundwater recharge through Vertisols: Irrigated Cropland vs. Natural Land, Israel. Vadose Zone J. 10, 662–674. http://dx.doi.org/10.2136/vzj2010.0109.

Lorenz, D.W., Delin, G.N., 2007. A regression model to estimate regional ground water recharge. Ground Water 45 (2), 196–208. http://dx.doi.org/10.1111/j.17456584.2006.00273.x.

Marquardt, D.W., 1963. An algorithm for least-squares estimation of nonlinear parameters. J. Soc. Ind. Appl. Math. 11, 431–441. http://dx.doi.org/10.1137/0111030.

Mualem, Y., 1976. A new model for predicting the hydraulic conductivity of unsaturated porous media. Water Resour. Res. 12, 513–522. http://dx.doi.org/10.1029/WR012i003p00513.

Ng, G.-H.C., McLaughlin, D., Entekhabi, D., Scanlon, B., 2009. Using data assimilation to identify diffuse recharge mechanisms from chemical and physical data in the unsaturated zone. Water Resour. Res. 45, 1–18. http://dx.doi.org/10.1029/2009WR007831.

Nolan, B.T., Healy, R.W., Taber, P.E., Perkins, K., Hitt, K.J., Wolock, D.M., 2007. Factors influencing ground-water recharge in the eastern United States. J. Hydrol. 332, 187–205. http://dx.doi.org/10.1016/j.jhydrol.2006.06.029.

Nolan, B.T., Ma, L., Green, C.T., Bayless, R., Malone, R.W., 2010. Predicting unsaturated zone nitrogen mass balances in agricultural settings of the United States. J. Environ. Qual. 39, 1051–1065. http://dx.doi.org/10.2134/jeq2009.0310.

Rimon, Y., Dahan, O., Nativ, R., Geyer, S., 2007. Water percolation through the deep vadose zone and groundwater recharge: preliminary results based on a new vadose zone monitoring system. Water Resour. Res. 43, 1–12. http://dx.doi.org/10.1029/2006WR004855.

Rimon, Y., Nativ, R., Dahan, O., 2011a. Physical and chemical evidence for pore-scale dual-domain flow in the vadose zone. Vadose Zone J. 9, 1–10. http://dx.doi.org/10.2136/vzj2009.0113.

Rimon, Y., Nativ, R., Dahan, O., 2011b. Vadose zone water pressure variation during infiltration events. Vadose Zone J. 10, 1–10. http://dx.doi.org/10.2136/vzj2010.0061.

Ritter, A., Hupet, F., Muñoz-Carpena, R., Lambot, S., Van-clooster, M., 2003. Using inverse methods for estimating soil hydraulic properties from field data as an alternative to direct methods. Agric. Water Manage. 59, 77–96.

Schaap, M.G., Leij, F.J., van Genuchten, M.Th., 2001. ROSETTA: a computer program for estimating soil hydraulic parameters with hierarchical pedotransfer functions. J. Hydrol. 251, 163–176.

Sheffer, N.A., Dafny, E., Gvirtzman, H., Navon, S., Frumkin, A., Morin, E., 2010. Hydrometeorological daily recharge assessment model (DREAM) for the Western Mountain Aquifer, Israel: model application and effects of temporal patterns. Water Resour. Res. 46, W05510. http://dx.doi.org/10.1029/2008WR007607.

Šimůnek, J., Šejna, M., Saito, H., Sakai, M., van Genuchten, M.T., 2009. The HYDRUS-1D software package for simulating the one-dimensional movement of water, heat, and multiple solutes in variably-saturated media Version 4.08. Dep. Environ. Sci. Univ. of California, Riverside.

Smerdon, B.D., Allen, D.M., Neilsen, D., 2010. Evaluating the use of a gridded climate surface for modelling groundwater recharge in a semi-arid region (Okanagan Basin, Canada). Hydrol. Processes 24, 3087–3100. http://dx.doi.org/10.1002/hyp.7724.

Turkeltaub, T., Dahan, O., Kurtzman, D., 2014. Investigation of groundwater recharge under agricultural fields using transient deep vadose zone data. Vadose Zone J. 13 (4). http://dx.doi.org/10.2136/vzj2013.10.0176.

van Genuchten, M.T., 1980. A closed-form equation for predicting the hydraulic conductivity of unsaturated soils. Soil Sci. Soc. Am. J. 44, 892–898. http://dx.doi.org/10.2136/sssaj1980.03615995004400050002x.

Wang, T., Zlotnik, V.A., Šimunek, J., Schaap, M.G., 2009. Using pedotransfer functions in vadose zone models for estimating groundwater recharge in semiarid regions. Water Resour. Res. 45 (4), W04412. http://dx.doi.org/10.1029/2008WR006903.

Wohling, D.L., Leaney, F.W., Crosbie, R.S., 2012. Deep drainage estimates using multiple linear regression with percent clay content and rainfall. Hydrol. Earth Syst. Sci. 16, 563–572. http://dx.doi.org/10.5194/hess-16-563-2012.

Wöhling, T., Vrugt, J.A., Barkle, G.F., 2008. Comparison of three multiobjective optimization algorithms for inverse modeling of vadose zone hydraulic properties. Soil Sci. Soc. Am. J. 72, 305–319. http://dx.doi.org/10.2136/sssaj2007.0176.

Wollschläger, U., Pfaff, T., Roth, K., 2009. Field-scale apparent hydraulic parameterisation obtained from TDR time series and inverse modelling. Hydrol. Earth Syst. Sci. 13, 1953–1966.

Wu, J., Zhang, R., Yang, J., 1996. Analysis of rainfall-recharge relationships. J. Hydrol. 177, 143–160. http://dx.doi.org/10.1016/0022-1694(95)02935-4.